Springer

Journal of Mechanical Science and Technology 23 (2009) 36~44

Journal of
Mechanical
Science and
Technology

www.springerlink.com/content/1738-494x
DOI 10.1007/s12206-008-1010-8

Bone density aspects in the biomechanical behavior of ALIF using cylindrical cages and PSF †

Young Kim*

School of Mechanical Engineering, Hanyang University, Seoul, 133-791, Korea

(Manuscript Received February 22, 2008; Revised September 24, 2008; Accepted October 8, 2008)

Abstract

Cage subsidence and loosening increase with a decrease of bone density. Thus, the stabilization of spinal segments may be dependent on density of cancellous bone. The aim of this study was to investigate the effects of bone density on the biomechanical behavior of the ALIF with cylindrical cages and PSF. Nonlinear numerical analysis was carried out by means of finite element method, and various Young's moduli those have been described by the bone density were employed for the calculation. The range of motion was increased by 120% with decreasing of the density. Relative slip distance increased by 810% at the bone-cage interface and by 1750% at the bone-screw interface with a decrease of the density. Continuous cage subsidence, cage loosening, screw loosening and screw failure would occur particularly during an excessive flexion and/or an excessive axial rotation. The excessive low density would mainly cause pedicle-screw loosening due to the remarkable screw slip. In the case of excessively reduced density, therefore, further study is required in order to investigate how to improve the current PSF for the segmental stability.

Keywords: ALIF; PSF; Cylindrical cage; Bone stress; Relative slip

1. Introduction

Bone density of spinal segments varies with individuals and decreases with ages [1]. Low bone density leads to low bone strength that would allow a higher risk of cage subsidence and cage loosening in the lumbar interbody fusion by using titanium cages [1-3]. Bone density of adjacent vertebrae, thus, would be a significant factor for stabilization of spinal segments as reported by Lund et al. [4] and Jost et al. [5]. A decrease of the bone density in the stand-alone anterior lumbar interbody fusion (ALIF) leads to an increment of bone indentation and relative motion at the bone-cage interface in immediate postoperative state [6]. However, other age-related geometric or mechanical changes of lumbar spinal segments except bone density were not substantial in the change of the biomechanical behaviors [6]. Addition of pedicle screw fixation (PSF) to the stand-alone ALIF improves segmental stability as *in vitro* shown by Gerber et al. [7] and Lund et al. [4] and as analytically reported by Kim [8]. With a low density of the bone adjacent to PSF-screw, its failure may occur even under physiologic loadings. With aging, furthermore, density reductions of bone would decrease stability of spine segments. It is unclear, however, how the change of bone density near PSF-screw affects the segmental stability or/and interbody fusion of the bone-cage interface.

Bone failure and/or relative slip at the bone-cage interface can induce cage subsidence [9-10]. The bone failure beneath the cage during initial loadings of the immediate postoperative state represents the initial cage subsidence. Then, bone loss beneath the cage due to excessive relative slip at the interface would cause a continuous subsidence of the cage after

† This paper was recommended for publication in revised form by Associate Editor Young Eun Kim

*Corresponding author. Tel.: +82 2 488 2156, Fax.: +82 2 475 7567
E-mail address: ykima@hanmail.net

the initial subsidence. The median time of the continuous cage subsidence was 2.75 months with deviations from 0.25 to 8 months after surgery in the standalone ALIF with rectangular cages [11], with an average of 3.7 mm cage subsidence. Ray [12] reported in the PLIF with cylindrical cages about 1.0 mm cage subsidence.

The objective of the current study was to investigate the effects of bone density on the biomechanical behavior of the ALIF with cylindrical cages and PSF. Nonlinear numerical analysis of the ALIF model has been performed by finite element method. Various Young's moduli of bone were employed for the calculation. Plastic deformation and relative slip either at the bone-cage interface or at the bone-PSF screw interface were predicted. A decrease of bone density would allow cage loosening at the bone-cage interface and screw loosening at the bone-screw interface.

2. Materials and methods

Effects of bone density on the biomechanical behavior of human lumbar spine segments (L4-L5) were investigated by means of the finite element method. The segments were anteriorly stabilized by cylindrical cages, bone graft and PSF under static physiologic loads.

Five cases of Young's moduli were considered based on the density variations with aging or with individuals in both cancellous bone (CB) and posterior bony elements (PE) (Table 1). According to the literature [1-3], CB was classified into normal, slightly reduced and significantly reduced densities. Then, PE was also classified into severely reduced and excessively reduced densities together with the significantly reduced density of CB.

The bone materials including CB, PE, bony endplate and bone graft were assumed to be linearly elastic and perfectly plastic. As Drucker-Prager equivalent stress of bone reached at the yield strength as shown in Tables 1 and 2, perfect plastic yielding occurred. The yield strength was defined as multiplying Young's modulus by the compressive yield strain of 0.84% [3]. Plastic deformation (or failure) of bone was assumed to occur when the minimal principal strain [13] of bone was below –0.84%.

For finite element modeling, the geometric data of L4-L5 segments were based on the literature [14-16]. Details of all structures with relevant material properties have been employed from the previous studies [8]. The geometry of the ALIF has been assumed to be symmetric about its sagittal plane, as shown in the overall element mesh of Fig. 1. The material properties used in this analysis are shown in Table 2. In the finite element implementation (ANSYS, version 9.0, ANSYS Inc., Canonsburg, PA), the materials were assumed to be isotropic and homogeneous. CB, PE, bone graft, PSF and interbody cage were modeled as 3-D isoparametric eight-node solid elements with three translation degrees of freedom (DOFs) (Table 3). Cortical bone and bony end-plates were modeled as four-node shell elements with six DOFs including three rotations and three transitions. Despite the direct connection between the solid element and the shell element, there was little difference in the elastic deformation of this study under the physiologic loadings

Table 1. Five cases of Young's moduli based on the density variations with aging or with individuals in both cancellous bone (CB) and posterior bony elements (PE).

density status	cases	Young's moduli	yield strain [3]	yield strength	Density [3], g/cm^3	Density [2], g/cm^3	Density [1], g/cm^3
normal	200CB-3.5PE	200MPa CB 3.5GPa PE	0.84%	1.68 MPa * 29.4 MPa	0.085 -	0.33 1.06	0.15 -
slightly reduced	40CB-3.5PE	40 MPa CB 3.5GPa PE	0.84%	0.34 MPa 29.4 MPa	0.057 -	0.24 1.06	- -
significantly reduced	14CB-3.5PE	14 MPa CB 3.5GPa PE	0.84%	0.12 MPa 29.4 MPa	0.045 -	0.17 1.06	0.1 -
severely reduced	14CB-1.4PE	14 MPa CB 1.4GPa PE	0.84%	0.12 MPa 11.8 MPa	0.045 -	0.17 0.79	0.1 -
excessively reduced	14CB-0.43PE	14MPa CB 0.43GPa PE	0.84%	0.12 MPa 3.6 MPa	0.045 -	0.17 0.53	0.1 -

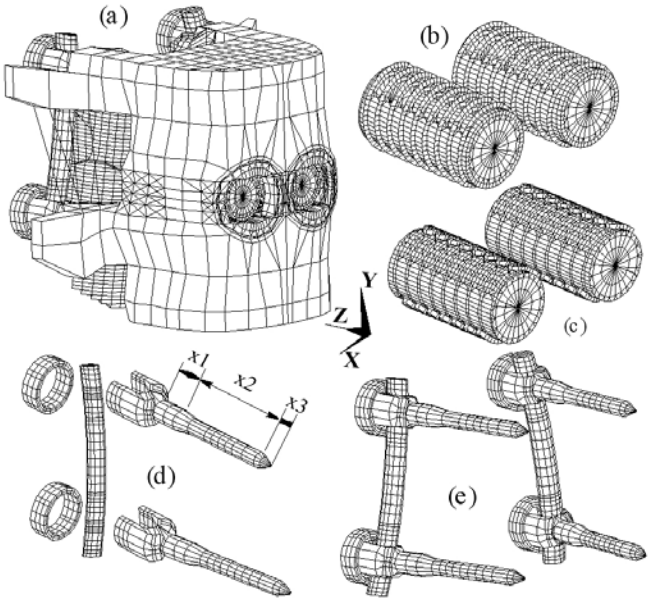

Fig. 1. A finite element model of the human lumbar interbody spine L4-L5 with paired cylindrical cages and PSF; (a) ALIF model, (b) cylindrical cages (TFC), (c) bone graft within the cages, (d) the screw, rod and nut of PSF and (e) assembled PSF.

between SOLID62 and SOLID73. SOLID62 was a nonlinear elstoplastic solid element type with 3 DOFs, whereas SOLID73 was a linear elastic solid element type with 6 DOFs.

The intervertebral disc had a uniform height of 11 mm and cross-sectional area of 1360 mm^2. The vertebral body was assumed to have 0.9 mm thick cortical outer shell with an internal cancellous core; however, the thickness of the bony end-plates was assumed to be 0.5 mm. Geometry for the facet joint was referred from Grobler et al. [14] and Panjabi et al. [16]. The annulus of the intervertebral disc was assumed to be a composite material with a series of fiber bands embedded in a matrix of ground substance. The annulus fibers and ligaments were modeled as cable elements supporting tension only. No muscle activation was considered in this study.

Two titanium interbody cages with outer diameter of 14 mm (including thread height 0.8 mm) and with length of 22.5 mm were inserted into a normal model of L4-L5 to simulate Ray TFC (Surgical Dynamics Inc, Concord. California) as shown in Fig. 1 (b). The cage was engaged into the bony end-plates with 0.7 mm depth. The bone graft packed firmly with bone chips was assumed to occupy every hole of the cage, as shown in Fig. 1 (c). Bone graft within the cage was assumed to have the properties of CB.

The contact areas between rod and screw, between bone and PSF screw, between bone and cage and between bone graft and cage were modeled as contact elements with an initial gap distance of zero and with a Coulomb friction coefficient of 0.4 [18]. The contact area of articulating facets was also modeled as contact elements with frictionless 0.45 mm initial gap. The elements are capable of supporting only compression in the normal direction and shear in the tangential direction to the surface. Slip distance was obtained by calculating slip length between two nodal points of a contact element. Gap distance was calculated by relative normal motion between two nodal points of a contact element. In the pedicle screw fixation (TSRH, Medtronic Sofamor Danek), screws, rods with lordosis and nuts were modeled as solid elements.

As shown in Fig. 1 (d), it was assumed that no relative motion occurs on the screw-bone interface of the middle (x2) due to the anchoring thread; however, relative motion occurs at the regions (x1 and x3) of the screw due to the relatively smooth surface. The diameter of the pedicle screw was assumed to be 6.0 mm at the region (x1) and 4.0 mm at the region (x2), on the basis of the sectional area of the PSF screw with 6.5 mm outer diameter (including thread height).

The inferior surface of the L5 vertebra was fixed in all degrees of freedom. Static loads were applied on the top surface of the human lumbar segments (L4-

Table 2. The material properties of the human lumbar spine (L4-L5) with cylindrical cages and PSF.

Materials	Young's modulus [MPa]	Yield strain [%], strength [MPa]	Poisson's ratio
Cortical bone [23] Bony end-plates	12000 12000	173 MPa 10 MPa	0.3
Cancellous bone [3]	14-200	0.84%	0.2
Posterior bone	430-3500	0.84%	0.25
Ground substance	4		0.49
Annulus fiber [15,24] Lateral Posterolateral Anterior Posterior	inner/middle/outer 76/106/136 59/70.5/82 76/106/136 59/70.5/82	Cross-sec. area (mm^2) 8.6/6.7/4.8 5.7/5.8/4.7 6.4/5.5/3.4 4.2/3.9/3.0	
Titanium cage, Posterior screw fixation	110,000	848.4	0.3
Bone graft	100	--	0.2
Ligaments [19,25]		Cross-sec. area (mm^2)	
Anterior longitudinal	7.8	22.4	
Posterior longitudinal	10	7.0	
Ligamentum flavum	17	14.1	
Transverse ligament	10	0.6	
Capsular ligament	7.5	10.5	
Intraspinous	10	14.1	
Supraspinous	8.0	10.5	

Table 3. The mesh structure of the finite element model.

Element types in ANSYS	No of elements and DOFs	Materials
Solid element (SOLID62)	31166, 3-DOFs (ux, uy, uz)	Cancellous bone, posterior bony elements, ground substance, cage, bone graft and PSF.
Contact element (CONTAC52)	7442, 3-DOFs (ux, uy, uz)	Top and bottom surfaces of the cage packed with bone graft, bone graft inside cage, screw-necks, screw-tips, contact between rod and screw.
Cable element (LINK10)	706, 3-DOFs (ux, uy, uz)	Annulus fibrosis, ligaments
Shell element (SHELL43)	1494, 6-DOFs (ux, uy, uz, rotx, roty, rotz)	Cortical bone (0.9 mm thickness), bony end-plate (0.5 mm thickness)

L5).

Loading conditions on the superior surface of L4 were chosen within a normal physiologic range [19] using axial rotation of 10 Nm, lateral bending of 5 Nm, and flexion/extension of 10 Nm. Compression on the lumbar segments is up to 1000 N for standing and walking and is higher during lifting [26]. Thus, a compressive preload of 1200 N was applied by uniformly distributed nodal vertical loads acting on the superior surface of L4.

Angular displacement and compressive preload were applied simultaneously on the superior surface that was the shell element with 6 DOFs. With a changed angular displacement on the surface, computation was repeated to get the additional moment of 10 Nm to the sagittal moment arising from the compressive preload [8], through 60-240 iterations depending on the loading conditions.

3. Results

As shown in Table 4, the axial compressive displacement on the superior surface of L4 increased with a decrease of CB density. The increase in the

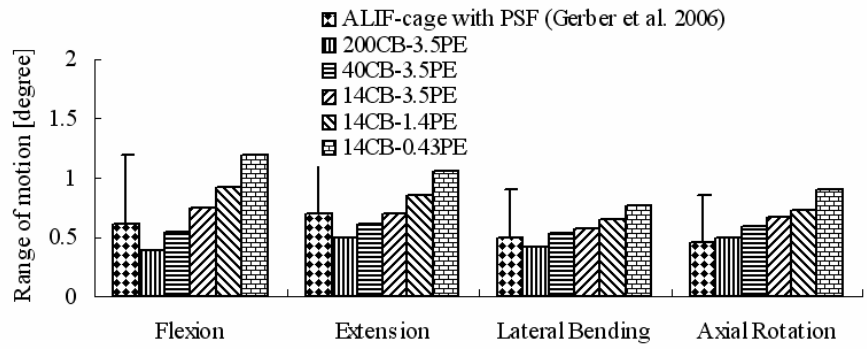

Fig. 2. The predicted ROM was compared with the experimental literature [7], which represents the mean ROM with a standard deviation. The ROM increased with a decrease of bone density.

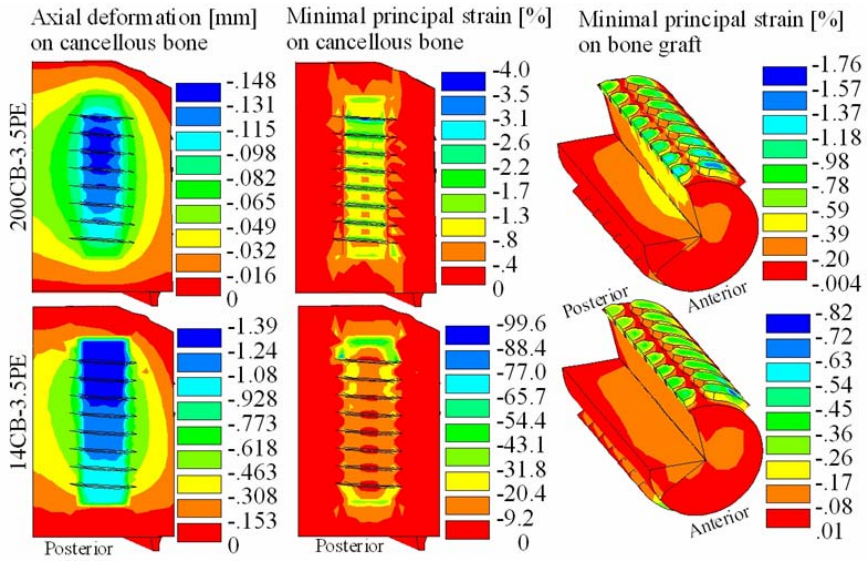

Fig. 3. The axial deformation and minimal principal strain of the case of 200CB-3.5PE were compared with those of 14CB-3.5PE during 1200 N axial compression.

displacement was more substantial than that of the cases with a decrease of PE density. Facet reaction increased during 10 Nm axial rotation with 1200 N preload as CB density decreased. Little reaction was predicted during all loadings except axial rotation.

ROMs were increased with decreasing both CB and PE densities as shown in Fig. 2. The ROMs were in the range of the experimental literature [7]. The excessively low bone density increased ROM by 120%.

Under 1200 N axial compression, the axial deformation of cancellous bone was much higher in the case of 14CB-3.5PE than in the case of 200CB-3.5PE (Fig. 3). The deformation was greater at the anterior region of the bone-cage interface than at the posterior region. The level of the minimal principal strain on cancellous bone in the case of 14CB-3.5PE was much

Table 4. The vertical displacement at the center of the superior surface of L4 under 1200 N compression and the facet reaction during 10 Nm axial rotation with 1200 N preload.

Young's moduli	Displacement [mm] during 1200 N preload	Facet reaction [N] during 10 Nm axial rotation with 1200 N preload
200CB-3.5PE	0.60	0.4
40CB-3.5PE	2.04	6.6
14CB-3.5PE	3.95	6.9
14CB-1.4PE	4.01	9.9
14CB-0.43PE	4.07	5.4

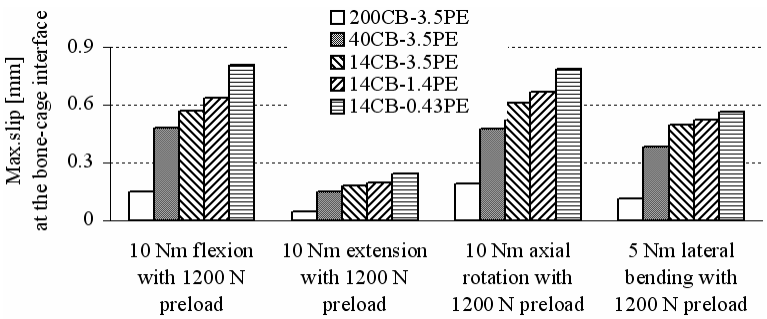

Fig. 4. The maximum slip distance was predicted at the bone-cage interface under the combined loadings.

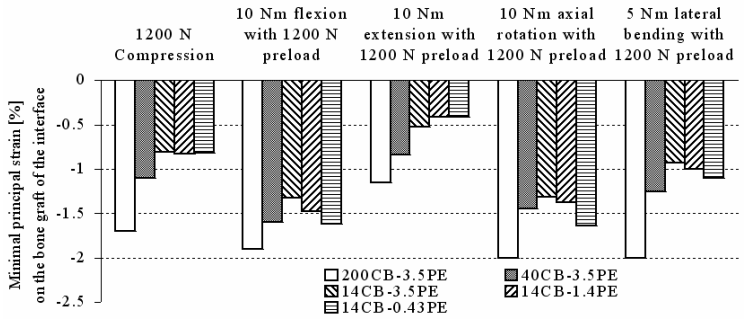

Fig. 5. The minimal principal strain of the bone graft was predicted.

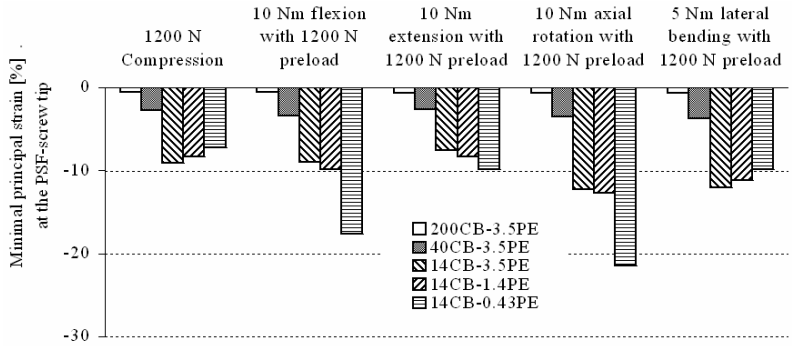

Fig. 6. The minimal principal strain of the bone near the screw-tip was predicted.

less than that of 200CB-3.5PE; on bone graft, however, the strain level of 14CB-3.5PE was greater than that of 200CB-3.5PE.

A decrease in either CB density or PE density caused a substantial increase up to 810% in the maximum slip distance of the bone-cage interface (Fig. 4). The level of the minimal principal strain on bone graft was increased with decreasing CB density (Fig. 5); on the bone near PSF-screw, however, the level of the strain decreased (Fig. 6). The maximum slip distance of the bone adjacent to PSF-screw tip substantially increased by 1750% as bone density decreases (Fig. 7).

Fig. 8 shows the maximum level of the equivalent stress in the middle of the PSF-screw. The stress level increased as CB density decreases; however, there was no substantial change in the stress level as PE density decreases. The level of the stress during flexion/axial rotation with 1200 N preload was about 2 times higher than that of 1200 N compression only.

4. Discussion

This study showed that a decrease of bone density in the ALIF by using cylindrical cages and PSF allowed a substantial increase in ROM, axial compres-

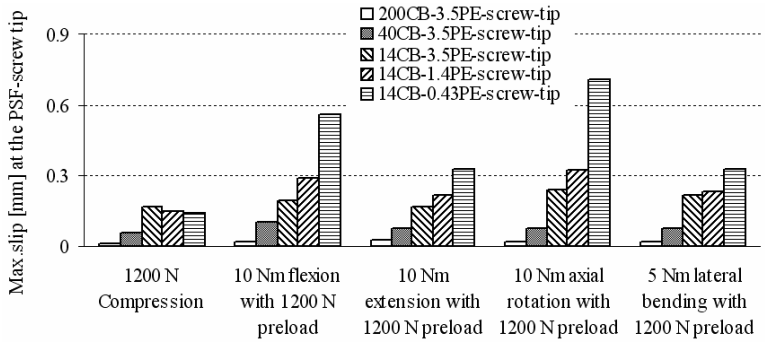

Fig. 7. The maximum slip distance was predicted at the screw tip-bone interface during all loadings with 1200 N preload.

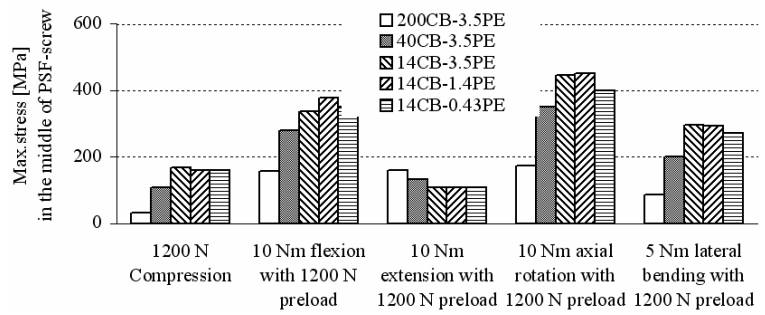

Fig. 8. The maximum equivalent stress of PSF-screw was predicted during the combined loadings.

sive displacement, plastic bone deformation and relative slip distance of either the bone-cage interface or the bone-screw interface. The greater plastic deformation and relative slip of the interfaces increased the risks of cage subsidence, cage loosening and screw loosening.

Clinically, either a rectangular or cylindrical cage was subsided in lumbar vertebrae during physiologic loading modes [11, 12]. The bone beneath the cage/the indentor failed and compacted [9]. The bone surrounding the cage would be compacted/densified repeatedly in the axial direction during physiologic loadings until the maximum level of the bone stress is less than the yield strength. Then, no more plastic deformation of bone would occur under small relative slip distance of the bone-cage interface. The cage subsidence would, therefore, be related to the plastic deformation of bone and slip distance at the interface. In the current study, the plastic deformation of bone materials was predicted by the minimal principal strain. The plastic deformation represents local bone failure. The plastic deformation and slip distance at the bone-cage interface increased with a decrease of either CB density or PE density. As well, the decrease of the density increased the plastic deformation and slip distance of the bone-screw interface. The greater slip distance at the bone-screw interface showed the greater slip distance at the bone-cage interface, particularly during axial rotation/flexion as shown in Figs. 4 and 7. The greater plastic deformation and slip distance at both interfaces showed the higher risks of cage subsidence, cage loosening, screw loosening and screw failure.

Bone graft. Bone graft within the cage can be compressed in a normal case of CB density because the level of the minimal principal strain was less than –0.84% [3]. A reduced density in either CB or PE, however, would not allow the failure of bone graft due to a higher level of the minimal principal strain as compared to –0.84%. Then, the bone graft would be incorporated into the new bone matrix formed during fusion. The regions with the range of tensile and compressive strains (±0.1%) would not allow the initial formation or later maintenance of bone inside the cages. With a decrease in either CB or PE density, therefore, a new bone matrix instead of the plastic deformation would be formed on the bone graft, together with the fact that relative slip distance at the bone graft-cage interface was so small.

Screw loosening. Stress/strain concentration was

found at the bone adjacent to the tip of the PSF-screw. At the bone the level of the minimal principal strain was greater than yield strain of -0.84% in the case of 200CB-3.5PE, but much below -0.84% in the case of 14CB-3.5PE. In the cases of a reduced PE density, the slip distance of the bone-screw interface was greater than 0.15 mm [10]. In the case of 14CB-0.43PE, in particular, the strain level and relative slip distance were so excessive that screw loosening would occur at the interface during flexion and/or axial rotation. Furthermore, the reduced PE density allowed a substantial increase in the relative slip distance of the bone-cage interface.

Limitations. In the case of the stand-alone ALIF, Kim [6] showed analytically that a significant increase of slip distance occurs as CB density decreases. In the current study using the ALIF with PSF, five cases of Young's moduli were considered based on the variations of bone density. The results of the case of 200CB-3.5PE represented the biomechanical behaviors of interbody fusion with a uniform bone density of middle age. 14CB-0.43PE was, however, assumed to be a case of old age with the lowest bone density in both CB and PE. It is unclear *in vivo* that the reduction in PE density initiates whether together with or after the reduction in CB density. However, CB density decreased by about 50% with aging [1-3] and then additional reduction of PE density was considered in the current study. The level of the yield strain in PE is little known whereas the level of the yield strain in CB was likely to be constant despite the variations of its density [3]. The level of the yield strain in PE was assumed to be the same as that of CB in the current study. In addition, the muscle was not included in the current model. Instead, an increased compressive force of 1200 N due to the addition of muscle forces was applied on the model. Trunk muscle activation caused a follower load on the spinal curve so that lumbar spine supports compressive loads of physiologic magnitudes without buckling of the spine [27].

In conclusion, an excessively low bone density could allow 120% increase of ROM, 810% increase of cage slip and 1750% increase of pedicle-screw slip. The excessive low density would mainly increase the risk of pedicle-screw loosening due to the remarkable increase of screw slip. Particularly continuous cage subsidence, cage loosening, screw loosening and screw failure would occur during an excessive flexion and/or an excessive axial rotation. In the case of excessively reduced density, further study is required in order to investigate how to improve PSF for the segmental stability.

References

[1] Le. Mosekilde, Le Mosekilde and C. C. Danielsen, Biomechanical Competence of Vertebral Trabecular Bone in Relation to Ash Density and Age in Normal Individuals, *Bone* 8 (1987) 79-85.

[2] D. R. Carter and W. C. Hayes, The Compressive Behavior of Bone as a Two-Phase Porous Structure, *J Bone & Joint Surg* 59 (1977) 954-962.

[3] D. L. Kopperdahl and T. M. Keaveny, Yield strain behavior of trabecular bone, *J. Biomech* 31 (1998) 601-608.

[4] T. Lund, T. T. Oxland, B. Jost, P. Cripton, S. Grassmann, C. Etter and L. P. Nolte, Interbody cage stabilization in the lumbar spine: biomechanical evaluation of cage design, posterior instrumentation and bone density, *J Bone Joint Surg Br* 80 (1998) 351-359.

[5] B. Jost, P. A. Cripton, T. Lund, T. T. Oxland, K. Lippuner, P. Jaeger and L. P. Nolte, Compressive strength of interbody cages in the lumbar spine: the effect of cage shape, posterior instrumentation and bone density, *Eur Spine J* 7 (1998) 132-141.

[6] Y. Kim, Prediction of Mechanical Behaviors at Interfaces between Bone and Two Interbody Cages of Lumbar Spine Segments, *Spine* 26 (13) (2001) 1437-1442.

[7] M. Gerber, N. R. Crawford, R. H. Chamberlain, M. S. Fifield, J. C. LeHuec, C. A. Dickman, Biomechanical Assessment of Anterior Lumbar Interbody Fusion with an Anterior Lumbosacral Fixation Screw-Plate: Comparison to Stand-Alone Anterior Lumbar Interbody Fusion and Anterior Lumbar Interbody fusion with Pedicle Screws in an Unstable Human Cadaver Model, *Spine* 31 (7) (2006) 762-768.

[8] Y. Kim, Finite Element Analysis of Anterior Lumbar Interbody Fusion; Threaded Cylindrical Cage and Posterior Pedicle Screw Fixation, *Spine* 32 (23) (2007) 2558-2568.

[9] J. S. Tan, C. S. Bailey, M. F. Dvorak, C. G. Fisher, T. R. Oxland, Interbody device shape and size are important to strengthen the vertebra-implant interface, *Spine* 30 (6) (2005) 638-644.

[10] R. M. Pilliar, H. U. Cameron, R. P. Welsh and A. G. Binnington, Radiographic and Morphologic

Studies of Load-bearing Porous-surfaced Structured Implants, *Clinical Orthopaedics and Related Research* 156 (1981) 249-257.

[11] J. Y. Choi and K. H. Sung, Subsidence after anterior lumbar interbody fusion using paired stand-alone rectangular cages, *Eur Spine J* 15 (2006) 16-22.

[12] C. D. Ray, Threaded titanium cages for lumbar interbody fusions. *Spine* 22 (1997) 667–79.

[13] T. H. Smit, A. Odgaard and E. Schneider, Structure and function of vertebral trabecular bone, *Spine* 22 (24) (1997) 2823-2833.

[14] L. J. Grobler, P. A. Robertson, J. E. Novotny, M. H. Pope, Etiology of Spondylolisthesis: Assessment of the Role Played by Lumbar Facet Joint Morphology, *Spine* 18 (1) (1993) 80-91.

[15] F. Marchand and A. M. Ahmed, Investigation of the Laminate Structure of Lumbar Disc Annulus Fibrosis, *Spine* 15 (5) (1990) 402-410.

[16] M. M. Panjabi, V. K. Goel, K. Takata, J. Duranceau, M. Krag and M. Price, Human Lumbar Vertebrae - Quantitative Three-Dimensional Anatomy, *Spine* 17 (1992) 299-306.

[17] M. M. Panjabi, T. Oxland, K. Takada and V. K. Goel, Duranceau J and Krag M. Articular Facets of the Human Spine: Quantitative Three-Dimensional Anatomy, *Spine* 18 (10) (1993) 1298-1310.

[18] A. Shirazi-Adl, M. Dammak and G. Paiement, Experimental Determination of Friction Characteristics at the Trabecular Bone/Porous-coated Metal Interface in Cementless Implants, *Journal of Biomedical Materials Research* 27 (1993) 167-175.

[19] A. A. White and M. M. Panjabi, *Clinical Biomechanics of the Spine*. JB Lippincott, Philadelphia, 2ed, pp.20-28, 106-112 (1990).

[20] E. K. Antonsson and R. W. Mann, Frequency content of gait. *J Biomech* 18 (1985) 39-47.

[21] L. E. Lanyon and C. T. Rubin, Static versus dynamic loads as an influence on bone remodeling. *J Biomech* 17 (1985) 897-900.

[22] C. T. Rubin and L. E. Lanyon, Regulation of bone formation by applied dynamic loads. *J Bone & Joint Surg* 66A (1984) 397-402.

[23] S. C. Cowin, *Bone Mechanics* (2ed), CRC Press, Inc. Boca Raton, Florida (1991).

[24] D. L. Skaggs, M. Weidenbaum, J. C. Latridis, A. Ratcliffe and V. C. Mow, Regional Variation in Tensile Properties and Biochemical Composition of the Human Lumbar Annulus Fibrosis, *Spine* 19 (12) (1994) 1310-1319.

[25] A. Nachemson and J. Evans, Some mechanical Properties of the Third Lumber Inter-laminar Ligament [ligamentum flavum], *J Biomech* 1 (1968) 211.

[26] A. Nachemson, Lumbar Intradiscal Pressure, in: *The Lumbar Spine and Back Pain*, M.I.V. Jayson, ed., Chap 9, 191-203.

[27] A. G. Patwardhan and K. P. Meade, A Frontal Plane Model of the Lumbar Spine Subjected to a Follower Load: Implications for the Role of Muscles, ASME, *J Biomecha Engr*, 123 (3) (2001), 212-217.

Young Kim received a B.S. degree in Mechanical Engineering from Chonnam National University in 1986. He then went on to receive his M.S. from KAIST and Ph.D. degrees from University of Wisconsin-Madison in 1991 and 1996, respectively. Dr. Kim has a lot of industrial experiences over 10 years (1996~2006). Dr. Kim is currently a Research Professor at the School of Mechanical Engineering at Hanyang University in Seoul, Korea. Dr. Kim's research interests are in the area of spinal biomechanics, mechanical design, product design, environmental machinery design, application of porous materials and ballistic impacts.